

Chemical Functionalization of Bioceramics To Enhance Endothelial Cells Adhesion for Tissue Engineering

Françoise Borcard,[§] Davide Staedler,[§] Horacio Comas,[§] Franziska Krauss Juillerat,[†] Philip N. Sturzenegger,[†] Roman Heuberger,[#] Urs T. Gonzenbach,[†] Lucienne Juillerat-Jeanneret,^{*,‡} and Sandrine Gerber-Lemaire^{*,§}

[§]Institute of Chemical Sciences and Engineering, EPFL, CH-1015, Lausanne, Switzerland

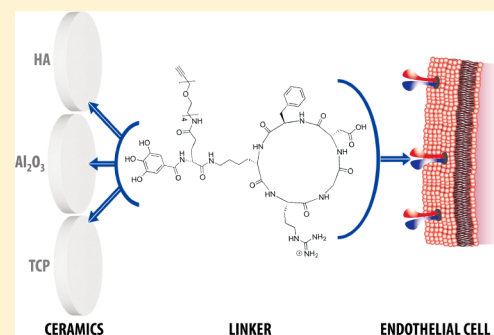
[†]Nonmetallic Inorganic Materials, ETHZ, CH-8093 Zürich, Switzerland

[#]RMS Foundation, CH-2544 Bettlach, Switzerland

[‡]University Institute of Pathology, CHUV-UNIL, CH-1011, Lausanne, Switzerland

Supporting Information

ABSTRACT: To control the selective adhesion of human endothelial cells and human serum proteins to bioceramics of different compositions, a multifunctional ligand containing a cyclic arginine-glycine-aspartate (RGD) peptide, a tetraethylene glycol spacer, and a gallate moiety was designed, synthesized, and characterized. The binding of this ligand to alumina-based, hydroxyapatite-based, and calcium phosphate-based bioceramics was demonstrated. The conjugation of this ligand to the bioceramics induced a decrease in the nonselective and integrin-selective binding of human serum proteins, whereas the binding and adhesion of human endothelial cells was enhanced, dependent on the particular bioceramics.



INTRODUCTION

The development of cellularized bone implants is a promising approach for the treatment of large bone defects. A limitation associated with large bone substitutes is the ability to develop a functional vascular system. The vascularization of implants is required to ensure the formation of stable and functional structures and to provide nutrients to the cells of the implants.¹ Different strategies can be applied to allow the vascularization of implants, which include the incorporation of pro-angiogenic growth factors into the biomaterials,^{2–7} the generation of pro-angiogenic materials mimicking the extracellular matrix,^{8–10} and the preseeding of endothelial cells in the implants prior to implantation.^{11–13} The arginine-glycine-aspartate (RGD)-based peptide sequences are widely used for the recognition of integrins to selectively target endothelial cells. In particular, cyclic RGD peptides are specific ligands for $\alpha_v\beta_3$ integrins which are highly expressed by human endothelial cells and are involved in the adhesion of human endothelial cells to bioceramics.^{14,15}

Our approach explores methodologies to enhance the adhesion of human endothelial cells to biocompatible ceramics for further applications in tissue engineering.¹⁶ We recently demonstrated the ability of pyrogallol and catechol moieties to ensure stable anchoring of organic molecules on alumina bioscaffolds through complexation of the aluminum present in the inorganic matrix.¹⁷ We disclose herein the surface modification of bioceramics of different chemical composition with organic ligands containing the *cyclo*[Arg-Gly-Asp-D-Phe-

Lys] (cRGDfK) unit linked to a gallate functionality through an ethylene glycol spacer. The chemical functionalization of the bioceramics was monitored by X-ray photoelectron spectroscopy (XPS). Three different bioceramics, i.e., aluminum oxide (alumina), tricalcium phosphate (TCP), and hydroxyapatite (HA), were investigated. HA was used as a reference material as it is a highly studied bioscaffold and human umbilical vein endothelial cells (HUVEC) as an endothelial cell model to evaluate the adhesive properties and biocompatibility of the bioceramics functionalized with the cRGDfK-gallate ligand.

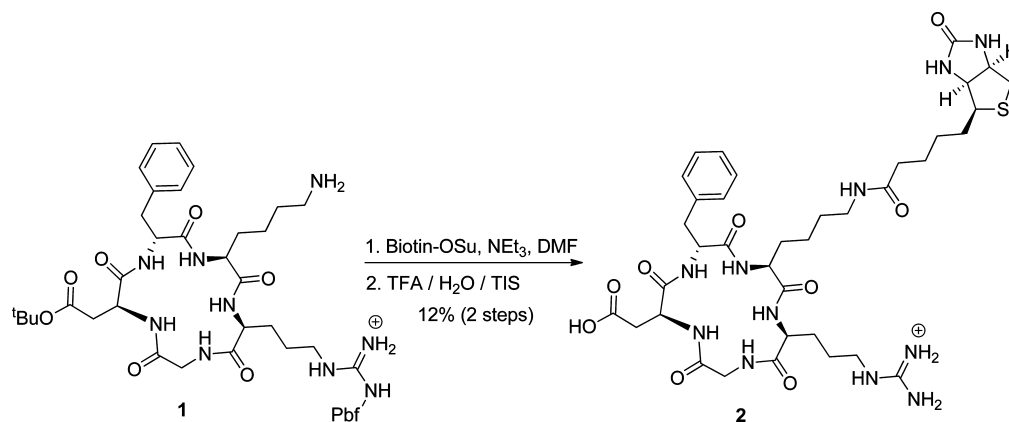
RESULTS

Synthetic Pathways toward Organic Ligands for the Functionalization of Bioceramics. *Synthesis of Compound 2.* A model compound containing the cRGDfK peptide conjugated to biotin was first prepared, in order to ascertain that human endothelial cells are able to recognize the cRGDfK peptide modified on the lysine residue. The synthesis started by a coupling reaction between a protected *c(t-Bu)RG(Pbf)DfK* peptide **1** (Supporting Information) obtained by solid-phase peptide synthesis using Fmoc protected amino acids¹⁸ and a OSu-activated biotin, in DMF at room temperature (rt) in the presence of triethylamine. Cleavage of all protecting moieties under acidic conditions and sequential washings with water,

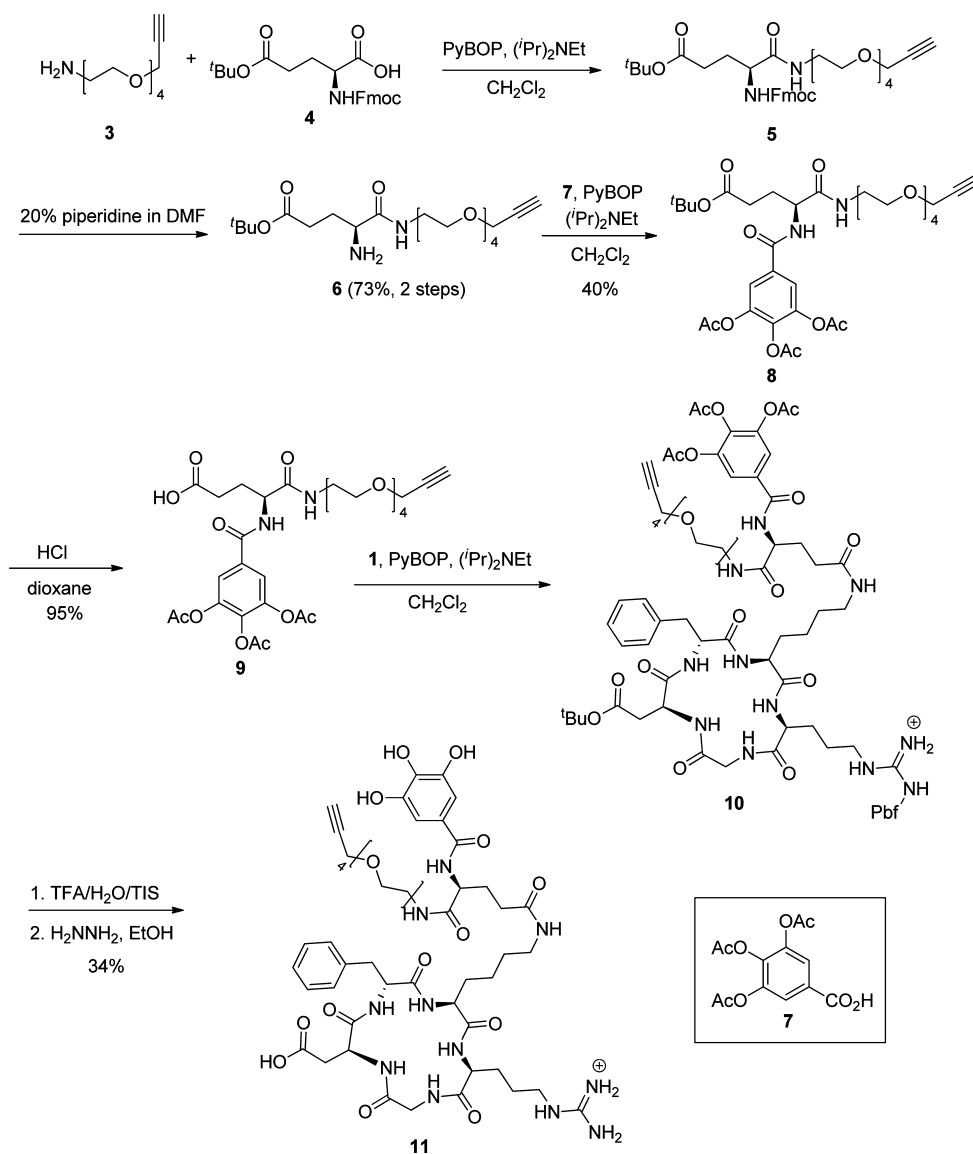
Received: April 30, 2012

Published: August 16, 2012

Scheme 1. Synthesis of Compound 2



Scheme 2. Synthesis of the Multifunctional Ligand 11



methanol, and dichloromethane provided the desired compound 2 (Scheme 1).

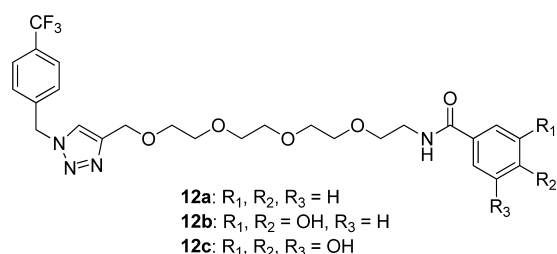
Synthesis of the Multifunctional Ligand 11. A chemical ligand containing the cRGDFK recognition entity and a gallate

moiety to allow conjugation to the bioceramics was synthesized. PEG derivative 3 was coupled with a *t*-Bu-semiprotected glutamic acid 4 in the presence of PyBOP as a coupling reagent as previously described¹⁶ to afford amide 5,

which was subsequently treated with piperidine to give amine **6** in 73% yield (two steps). Coupling with triacetoxy gallic acid **7** in the presence of PyBOP delivered intermediate **8** in moderate yield. The *tert*-butyl ester was cleaved under acidic conditions to liberate the carboxylic acid **9** which was reacted with protected peptide **1** in the presence of PyBOP and (*i*-Pr)₂NEt. Sequential cleavage of the peptide protecting moieties with TFA and deprotection of the three hydroxyl groups of the gallate entity with hydrazine provided the desired ligand **11**, which was purified by HPLC (Scheme 2).

Preparation and Characterization of the Ligand-Functionalized Bioceramics. Dense bioceramic disks from alumina, HA and TCP were prepared under pressure and sintering procedures. Then the bioceramics were functionalized with model ligands **12a–12c** bearing either pyrogallol or catechol moieties (Scheme 3). Using the methodology

Scheme 3. Chemical Structure of the Model Ligands 12a–12c^a



^aSynthesized as previously described in ref 17.

previously disclosed for the functionalization of alumina bioceramics with organic ligands,¹⁷ surface modification of HA and TCP bioceramics with compounds **12a–12c** was achieved through complexation of the calcium present in the inorganic matrix by two adjacent hydroxyl groups of the aromatic ring of catechol (**12b**) or pyrogallol (**12c**).

The functionalization of HA and TCP bioceramics with the ligands **12a–12c** was monitored by XPS, following incubation of the bioceramics with **12a–12c**, in water for 24 h. Surface analysis of the unfunctionalized (incubation with pure water) and of functionalized HA and TCP bioceramics was performed by XPS to determine the atomic composition of the samples. As previously shown for alumina bioceramics,¹⁷ ligand **12a** did not show significant binding to HA and TCP bioceramics. The peaks corresponding to fluorine and nitrogen atoms present in the ligands are only visible for the bioceramics which were treated with ligands **12b** or **12c** (Figure 1). Moreover the binding energy of fluorine (688 eV) is consistent with a C–F bond.

Thus, as previously observed with alumina-based bioceramics,¹⁷ the functionalization of HA and TCP bioceramics only occurred with ligands bearing catechol or pyrogallol groups (compounds **12b** and **12c**). Only the peaks corresponding to the initial composition of the bioceramics were observed for the bioceramics incubated with water or with **12a** (Table 1).

Cell Assays. Recognition of Ligands **2 and **11** by HUVEC.** First, the expression of $\alpha_v\beta_3$ integrin by HUVEC was demonstrated by immunofluorescence, using human lung A549 cells as $\alpha_v\beta_3$ integrin-negative control cells (Figure 2A,B). The selective interaction between compound **2** and integrins was proved by immunostaining of vinculin and cytoskeletal actin after incubation of the HUVEC in the

absence or the presence of compound **2** (Figure 2C,D), since the interaction of the integrin with its ligand will modify the cytoskeletal network.¹⁹ The colocalization of actin fibers and vinculin demonstrated the specific interaction between compound **2** and cellular integrins. Then the HUVEC were exposed to either free biotin as a negative control or to increasing concentrations (2.5, 5, 10 μ M) of compound **2** for assessing the recognition of this modified cRGDFK peptide by the integrins expressed by the treated cells. The HUVEC were first exposed to compound **2** for 30 min and then treated with Alexafluor-labeled streptavidin to visualize the presence of the biotin residue from compound **2** by fluorescence microscopy (Figure 2E,F). This experiment confirmed the recognition of compound **2** by the HUVEC, thus proving that the modification of the lysine residue of cRGDFK is not detrimental to the affinity toward integrins. Then the HUVEC were exposed to the ligand **11** under similar experimental conditions (Figure 2G,H), demonstrating that ligand **11** was efficiently recognized by the HUVEC integrins (Figure 2H). This ligand was thus further investigated for the functionalization of the bioceramics.

Chemical Functionalization of the Bioceramics and Adhesion of HUVEC. The HA, TCP, and alumina bioceramics were functionalized with ligand **11** under the same experimental conditions as for the model ligands **12a–12c**. Then the HUVEC (10⁶ cells per bioceramic) were added to either unfunctionalized or bioceramics functionalized with ligand **11**, for 2 h at 37 °C. After the washing and fixation steps, the cells were stained with crystal violet. HUVEC adhesion to the bioceramics was imaged with a stereomicroscope and the surface area of the adhered cells was quantified by the Image J software. First, the number of adhered HUVEC was compared among the different unfunctionalized bioceramics. Quantification of the number of adhered cells showed that alumina bioceramics had better adhesive properties for the HUVEC than HA or TCP bioceramics (results not shown). Then, quantification of the number of adhered HUVEC on the functionalized bioceramics was performed. After functionalization with ligand **11**, the number of adhered HUVEC on HA bioceramic significantly decreased, even at low concentrations of the ligand, compared to unfunctionalized HA bioceramic (Figure 3A). However, functionalization with ligand **11** at 2.5 μ M concentration resulted in the largest cell surface area, compared with unfunctionalized HA bioceramics and functionalized HA bioceramics with higher ligand concentrations (Figure 3B). Functionalization of TCP bioceramics with ligand **11** resulted in a significant increase of HUVEC adhesion to the bioceramic, both in terms of the number of adhered cells and of cell surface area (Figure 3C,D). The optimal concentration of ligand **11** was 5 μ M for the functionalization of the TCP bioceramics. At higher concentration (10 μ M), a decrease in cell adhesion was observed. For alumina bioceramics, the optimal ligand concentration for functionalization was 2.5 μ M. At higher concentrations of ligand **11**, HUVEC adhesion decreased (Figure 3E,F). Thus, the functionalization of alumina and TCP bioceramics with low concentration of ligand **11** induced an increase of both the number of adhered HUVEC and the cell size. For HA bioceramics, only the cell surface area was increased upon functionalization with ligand **11** at 2.5 μ M.

Adsorption of Human Serum Proteins on the Bioceramics. The adsorption of human blood proteins onto the three unfunctionalized or functionalized bioceramics was also

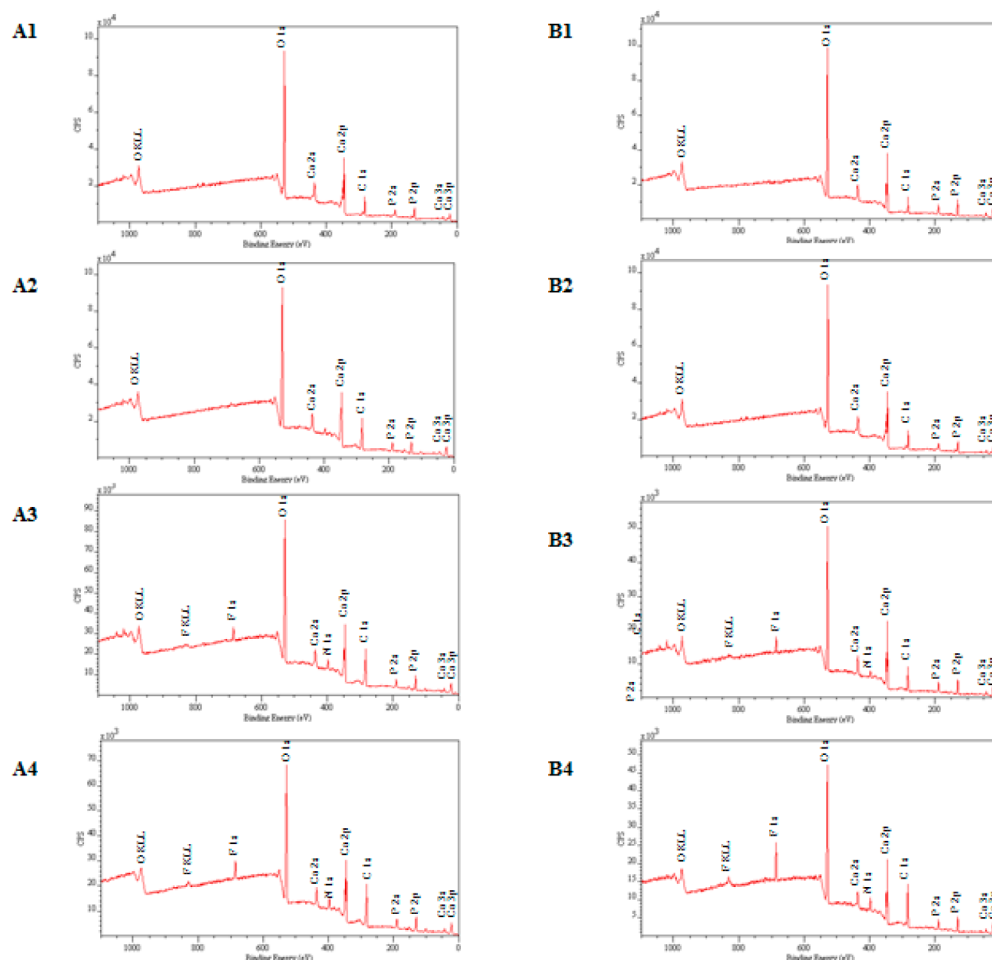


Figure 1. XPS spectra of unfunctionalized and functionalized bioceramics. XPS spectra for HA and TCP bioceramics incubated with water (A1-B1) or compound **12a** (A2-B2), **12b** (A3-B3), and **12c** (A4-B4).

determined. After incubation of the different bioceramics with human serum for 1 h at 37 °C, the bioceramics were extracted in boiling SDS buffer, and the proteins were resolved by electrophoresis and analyzed by Western blotting using specific antibodies. Functionalization of the bioceramics with the optimal concentrations of ligand **11** (previously determined through the evaluation of HUVEC adhesion) resulted in a decrease of the binding of vitronectin, fibronectin, and fibrinogen, which are involved in cell adhesion (Figure 4). The adhesion of IgG and other serum proteins (Supporting Information, Figure S1) was also decreased on the functionalized bioceramics. Alumina and TCP bioceramics adsorbed larger amounts of proteins compared to HA bioceramic.

Stability of the Chemical Coating on Bioceramics in Cell Culture Medium. Samples of HA, TCP, and alumina bioceramics, functionalized with compound **12c**, were incubated in Dulbecco's Modified Eagle medium (DMEM) supplemented with 10% fetal calf serum (FCS) for periods of 1 day and 14 days. The same experiment was performed on unfunctionalized samples of HA, TCP, and alumina bioceramics. Stability of the chemical functionalization over the time was monitored by XPS analysis of the surface of the bioceramic samples (Supporting Information, Table S1). After 14 days of incubation, partial release of the chemical coating was observed for HA bioceramics (monitored by the percentage of fluorine and nitrogen atoms). The coating of

TCP and alumina bioceramics was highly stable and was not affected by incubation for 14 days in cell culture medium.

DISCUSSION

Implant vascularization is a major challenge in tissue engineering, tissue repair, and regenerative medicine. Failure to develop a functional vasculature in large implants results in poor survival of the cells which should colonize the implant. Different approaches can be used to improve vascularization processes, including the delivery over time of soluble pro-angiogenic factors or the preintegration within the implant of vascular cells. In this study, a general method for the coating of bioceramics with ligands containing a targeting peptide for $\alpha_v\beta_3$ and $\alpha_v\beta_5$ integrins (cRGDfK) and an anchoring unit was developed. This surface functionalization enhanced both the number of human endothelial cells adhering to the materials and their spreading on the surface. The use of pyrogallol or catechol moieties allowed the efficient anchoring of the chemical ligands to the surface of HA, TCP, and alumina bioceramics, as demonstrated by the binding of compounds **12b** and **12c** to these materials. After simple incubation of the bioceramics with aqueous solutions of the ligands **12b** and **12c**, XPS analysis of the resulting surfaces demonstrated the stable coating of HA and TCP bioceramics. Complexation of the calcium present in the inorganic matrix is most likely involved in the coating process. Confirming previous data obtained with alumina bioceramics,¹⁷

Table 1. Atomic Composition of the Bioceramics Functionalized by Compounds 12a, 12b, or 12c^a

	atomic concentrations [%]			
	water	12a	12b	12c
HA Bioceramic				
F 1s	0.0	0.0	1.8	3.1
O 1s	55.3	50.4	48.8	39.7
N 1s	0.0	0.0	2.8	4.6
Ca 2p	16.1	12.7	12.2	8.0
C 1s	28.7	34.9	34.5	44.5
TCP Bioceramic				
F 1s	0.0	0.0	2.9	6.1
O 1s	58.9	55.8	52.6	41.1
N 1s	0.0	0.0	2.1	4.8
Ca 2p	16.3	16.9	14.1	10.2
C 1s	24.8	27.3	28.4	37.8
Alumina Bioceramic				
F 1s	0.0	0.0	6.4	7.4
O 1s	51.7	51.6	35.2	24.2
N 1s	0.0	0.0	5.2	7.5
Ca 2p	3.8	4.3	1.9	1.0
C 1s	17.4	21.0	36.3	52.5
Al 2p	27.1	23.1	15.0	7.4

^aThe percentages of atomic concentrations were determined by XPS for HA, TCP and alumina bioceramics functionalized with the compound 12a, 12b, or 12c. The values previously obtained for alumina bioceramic¹⁷ have been included here for comparison.

the pyrogallol group was superior to catechol moiety for the functionalization of HA and TCP bioceramics and was thus selected for the design of the functionalizing ligand.

Cell adhesion is mediated, in part, by the interaction of integrins with RGD peptides.²⁰ In particular, cRGDfK binds specifically to $\alpha_v\beta_3$ and $\alpha_v\beta_5$ integrins which are highly expressed by angiogenic endothelial cells.²¹ The synthesis of a multifunctional ligand displaying a pyrogallol functionality for conjugation to the bioceramics and cRGDfK for targeting integrins at the surface of endothelial cells was thus envisaged. A convergent pathway, using glutamic acid as template for the sequential introduction of the binding units for both the bioceramics and human endothelial cells and of an alkynyl group allowing click-reaction with a fluorescent azido-containing label, provided efficient access to the multifunctional linker 11. Chemical modification of cRGDfK on the lysine ϵ amino group did not affect its specific affinity for the integrins expressed by the HUVEC, as demonstrated by the binding of ligands 2 and 11 to the cells after only 30 min incubation time. The HA, TCP, and alumina bioceramics were then functionalized with ligand 11 via simple incubation in aqueous medium. The adhesion and spreading of the HUVEC on the functionalized bioceramics were compared to unfunctionalized bioceramics. In the case of the HA bioceramic, the presence of ligand 11 decreased the adhesion of the HUVEC to the bioceramic in agreement with previously published information.^{14,15} However, at low concentration of ligand 11, the cell surface area was increased. It was previously hypothesized that caspase activation occurred with the engagement of the integrins, decreasing human endothelial cell survival.^{14,15} For TCP and alumina bioceramics, an increase in the number of adhered HUVEC and of the cell surface area was obtained upon functionalization of the bioceramics with ligand 11, with optimal ligand concentrations of 5 and 2.5 μM , respectively. At

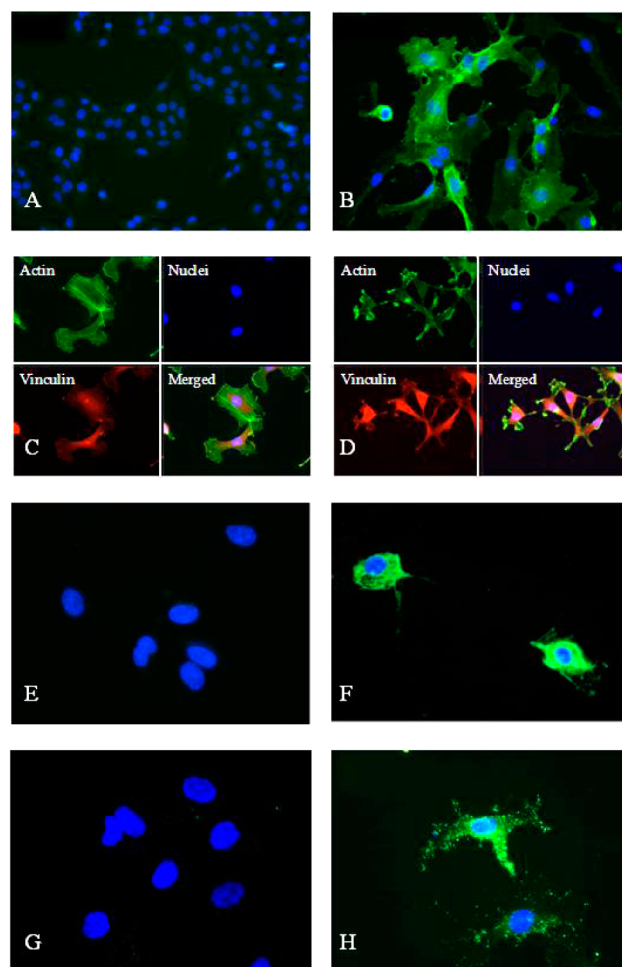


Figure 2. Binding of compounds 2 and 11 to HUVEC expression of the $\alpha_v\beta_3$ integrin by (A) A549 cells as negative control cells and (B) HUVEC. Expression of vinculin and actin by the HUVEC nonexposed (C) or exposed (D) for 45 min to compound 2 (5 μM). Nuclei were labeled in blue with DAPI. The HUVEC were exposed for 30 min to (E) free biotin (5 μM) as a control for nonspecific binding, or (F) to compound 2 (5 μM), then to fluorescent Alexafluor-labeled streptavidin to label biotin and to DAPI to label nuclei. The HUVEC were exposed for 3 h to (G) HBSS, or (H) to ligand 11 (5 μM) in HBSS, then to DAPI and Alexafluor-azide (10 μM) in the presence of CuSO_4 (2 mM) and sodium ascorbate (1 mM). Alexafluor-azide reacts with the alkyne moiety of ligand 11 through a click-reaction promoted by the combination of CuSO_4 and sodium ascorbate.

higher concentrations of ligand 11, both the number of adhered cells and the cell surface area decreased and became comparable to the values observed for unfunctionalized bioceramics. The different optimal concentrations determined for the three bioceramics suggest that the adhesion of endothelial cells is not only dependent on the nature of the chemical functionalization at the surface of the biomaterials, but also on the composition and topography of the materials.²² Consequently, comparable concentrations of the functionalizing ligand 11 do not have the same effect on the adhesion of the HUVEC on the three bioceramics evaluated.

The adsorption of human serum proteins onto unfunctionalized and functionalized bioceramics with ligand 11 was also determined. The functionalization of the bioceramics with ligand 11 decreased the adsorption of blood proteins able to

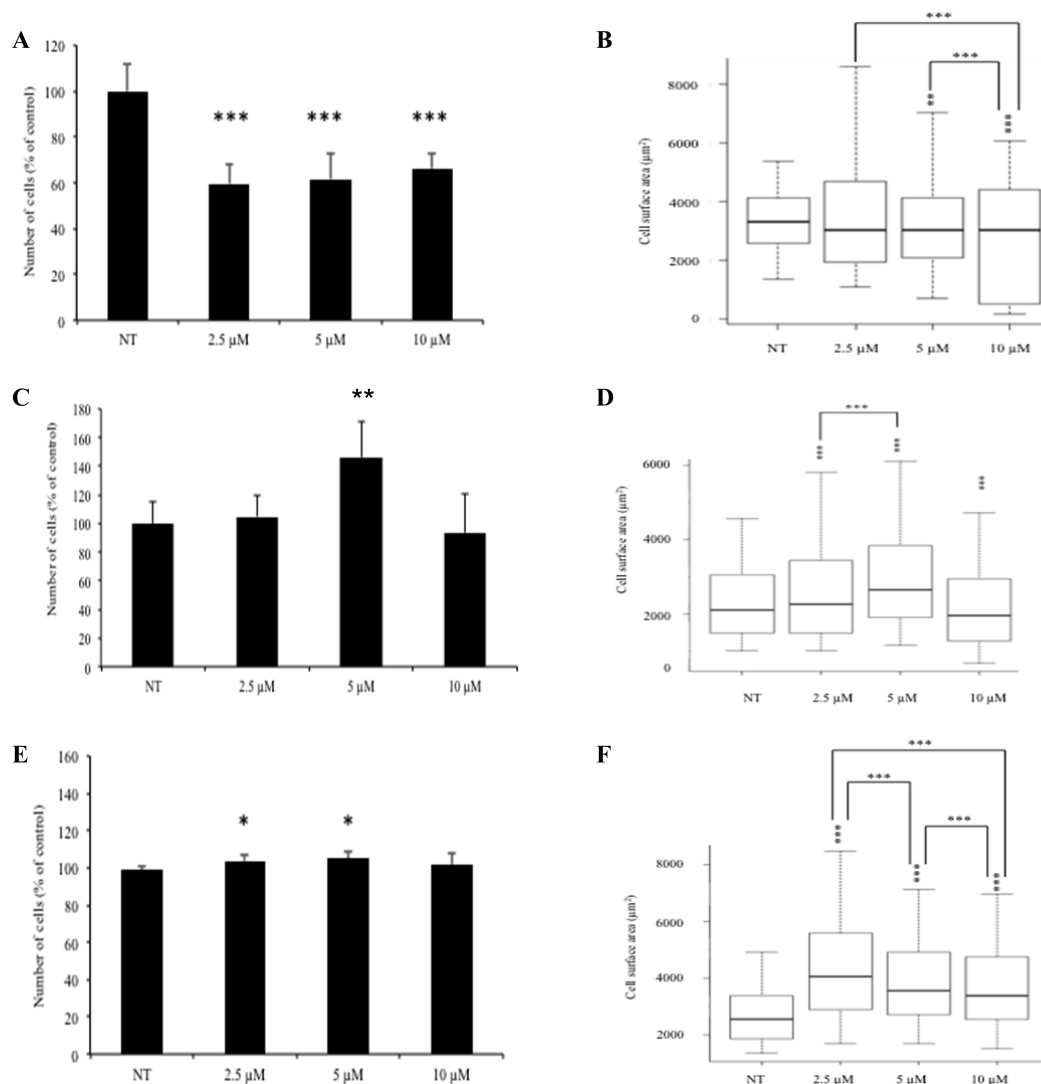


Figure 3. Adhesion of HUVEC to unfunctionalized and functionalized bioceramics. Disks of HA (A, B), TCP (C, D), and alumina (E, F) bioceramics functionalized with increasing concentrations (0–10 μM) of ligand **11** were incubated with HUVEC for 2 h in HBSS. The quantification of cell adhesion was performed by analysis of stereomicroscopy pictures (A, C, E). Results are the mean \pm SD of triplicates of three independent experiments. The number of cells adhering to the bioceramics disks was compared using a Student's *t*-test: *: $p < 0.05$; **: $p < 0.01$; ***: $p < 0.001$. The quantification of the surface areas of the adhered cells was performed using Image J software followed by a Boxplot representation (B, D, F). Cell surface areas on the bioceramics disks were compared using a Wilcoxon-signed rank test: *: $p < 0.05$; **: $p < 0.01$; ***: $p < 0.001$. (A, B) HA bioceramics; (C, D) TCP bioceramics; (E, F) alumina bioceramics.

bind integrins on the cell surface, such as vitronectin, fibronectin, and fibrinogen, which suggests good osteoconduction potential for the functionalized bioceramics,¹⁴ but also of immunoglobulins and serum albumin. TCP and alumina bioceramics adsorbed human proteins at higher levels than the widely used HA bioceramic, which represents interesting properties for some specific developments of implants for tissue engineering. In addition, chemical coating of TCP and alumina bioceramic is highly stable over the time (at least 14 days), which is promising for the long-term adhesion and proliferation of endothelial cells on the biomaterial.

CONCLUSION

The development of a functional vascular system in biomaterials for large permanent bone implants is a prerequisite to develop valid reconstruction materials allowing efficient tissue repair. The adhesion of endothelial cells on the biomaterials represents a challenge and is mandatory for the

formation of a functional vascular system. A general method for the functionalization of HA, TCP, and alumina bioceramics with organic ligands containing cRGDFK as integrin-recognition motif and a pyrogallol unit as anchoring moiety to bioceramics was developed. Surface modification of the bioceramics was ascertained by XPS analysis and the recognition of ligand **11** by human endothelial cells was demonstrated. The combination, in the same functionalizing ligand, of a targeting entity for the recognition of integrins with a pyrogallol anchoring unit for surface coating of the bioceramics and a reactive alkyne group for visualization, represents a promising tool to improve the adhesive properties of TCP and alumina bioceramics. The use of a pyrogallol moiety to ensure stable functionalization of the bioceramics provides an interesting strategy as surface modification is obtained by simple incubation in aqueous medium. The potential of TCP and alumina bioceramics to integrate human endothelial cells was significantly improved by functionalization with ligand **11**, as both the number and size of

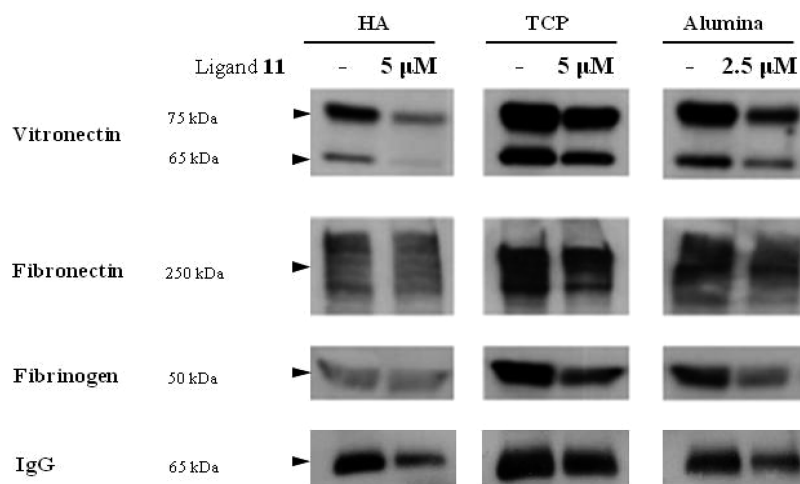


Figure 4. Adsorption of human serum proteins on the three bioceramics. Disks of HA, TCP, and alumina bioceramics either unfunctionalized or functionalized with ligand **11** were incubated with normal human serum for 1 h at 37 °C. The proteins adsorbed on the disks were extracted in SDS, resolved by electrophoresis and the presence of vitronectin, fibronectin, fibrinogen, and IgG was evaluated by Western blotting.

adhered endothelial cells were significantly higher than on unfunctionalized bioceramics. Moreover, the high stability of the chemical coating on TCP bioceramic over the time represents an additional asset for this biomaterial to be further developed for tissue engineering. The adhesion properties of HA bioceramic could not be improved by this method. A decrease of the adsorption of human serum proteins involved in cell adhesion was observed on the three functionalized bioceramics. However, functionalized alumina and TCP bioceramics demonstrated higher adsorption of human proteins than functionalized HA bioceramic, suggesting better biocompatibility of alumina and TCP bioceramics.

EXPERIMENTAL SECTION

General Procedures. Commercial reagents (Fluka, Aldrich, VWR, Switzerland) were used without further purification. Anhydrous solvents were obtained by filtration (PureSolv MD Series, Innovative Technology). TLCs for reaction monitoring were performed on Merck silica gel 60 F254 plates, and spots were revealed with UV light and reaction with KMnO_4 or ninhydrine. IR spectra were recorded on a Perkin-Elmer-1420 spectrometer. ^1H NMR spectra were recorded on a Bruker ARX-400 spectrometer (400 MHz) using CDCl_3 as solvent and calibrated using the solvent's residual signal at 7.27 ppm as an internal reference. ^{13}C NMR spectra were recorded on a Bruker ARX-400 spectrometer (100.6 MHz) using CDCl_3 as solvent and calibrated using the solvent's residual signal at 77.0 ppm as an internal reference. Chemical shifts are expressed in parts per million (ppm) and coupling constants (J) are in hertz. Mass spectra were obtained on a Nermag R-10-10C spectrometer with chemical ionization (NH_3) and mode m/z (amu) [% relative base peak (100%)]. Semipreparative HPLC was performed on a Waters Autopurification ZQ System equipped with a 2767 Sample Manager, a 2525 Binary Gradient Module and a 2996 Photodiode Array detector, coupled to Waters Micromass ZQ analyzer. The HPLC purifications were performed on XTerra Prep RP C18 (19×150 mm) columns, using reverse-phase conditions (2 to 100% acetonitrile with 0.1% TFA over 20 min). Purity of the synthesized compounds was determined by HPLC and ESI-HRMS. All compounds presented chemical purity > 95%. X-ray photoelectron spectroscopy (XPS) data were collected by Axis Ultra and Axis Nova instruments (Kratos analytical, Manchester, UK) under ultrahigh vacuum conditions ($<10^{-8}$ Torr) and using a monochromatic Al $K\alpha$ X-ray source (1486.6 eV). The source power was maintained at 225 or 150 W and the emitted photoelectrons were sampled from a $750 \mu\text{m} \times 300 \mu\text{m}$ area. The analyzer pass energy was 160 or 80 eV for survey spectra and 40 eV for high-resolution spectra. The adventitious carbon

1s peak was calibrated at 285 eV and used as an internal standard to compensate for any charging effects. Both curve fitting of the spectra and quantification were performed with the CasaXPS software, using relative sensitivity factors given by Kratos.

Chemical Syntheses. *Synthesis of cyclo[Arg-Gly-Asp-D-Phe-Lys]-Biotin (2).* *cyclo[Arg(Pbf)-Gly-Asp(OtBu)-D-Phe-Lys] 1* (40 mg, 0.04 mmol, 1 equiv) was dissolved in dry DMF in the presence of triethylamine (9 μL , 0.07 mmol, 1.5 equiv) and Biotin-OSu (17 mg, 0.05 mmol, 1.1 equiv). The reaction mixture was stirred overnight at rt. The product was concentrated under reduced pressure to remove the DMF. The residual product was dissolved in a solution of TFA/water (1 mL/0.06 mL) and triisopropylsilane (0.03 mL) was added. The reaction mixture was stirred at rt until total deprotection of the peptide. After concentration and sequential washings with water, methanol, and dichloromethane the desired product **2** was obtained as a white powder (mass: 4 mg, yield: 12% for 2 steps). IR (film): 3435, 1660, 1315, 1015, 950, 705, 645, 590, 520, 500 cm^{-1} . HRMS (ESI): (m/z): calcd for $\text{C}_{37}\text{H}_{56}\text{N}_{11}\text{O}_7\text{S}$ + H: 830.3983, found: 830.3965. $[\alpha]_{\text{D}}^{25} = -38$ ($c = 0.085$, CH_2Cl_2).

Synthesis of tert-Butyl N-3,6,9,12-tetraoxapentadec-14-yn-1-yl-N²-[[3,4,5-tris(acetyloxy)phenyl] carbonyl]-L- α -glutamate (8). *tert-Butyl N²-[9A fluoren-9-ylmethoxy]carbonyl]-N-3,6,9,12-tetraoxapentadec-14-yn-1-yl-L- α -glutamate 5* (865 mg, 1.4 mmol, 1 equiv) was dissolved in a solution of 20% piperidine in DMF at rt. The reaction mixture was stirred for 1 h at rt and concentrated under reduced pressure, and the intermediate product **6** was purified by flash column chromatography (DCM/MeOH (98:2)) (mass: 409 mg, yield: 74%). Acetoxygallic acid **7** (142 mg, 0.5 mmol, 1 equiv) and PyBOP (299 mg, 0.6 mmol, 1.2 equiv) were dissolved in dry DCM (2 mL). After 15 min, (*i*-Pr)₂NEt (0.12 mL, 0.7 mmol, 1.5 equiv) followed by a solution of *tert*-butyl-*N*-3,6,9,12-tetraoxapentadec-14-yn-1-yl-L- α -glutamate **6** (200 mg, 0.5 mmol, 1 equiv) in DCM (2 mL) were added to the reaction mixture. The reaction was stirred overnight at rt. The solvent was removed under reduced pressure and the product **8** was purified by flash chromatography (AcOEt/petroleum ether (7:1) to (9:1)) (mass: 134 mg, yield: 40%). IR (film): 3658, 3420, 3286, 2922, 1777, 1717, 1660, 1593, 1538, 1488, 1457, 1423, 1393, 1370, 1323, 1251, 1184, 1157, 1125, 1085, 1051, 949, 897, 833, 739, 615, 587, 555 cm^{-1} . ^1H NMR (400 MHz, CDCl_3): $\delta = 7.66$ (s, 2H, CH) 4.53 (m, 1H, CH), 4.23 (d, 2H, $^2J = 1.6$ Hz, CH_2), 3.71–3.38 (m, 16H, (CH_2)₆), 2.78–2.35 (m, 3H, CH, CH_2), 2.33 (s, 9H, (CH_3)₃), 2.30–2.09 (m, 2H, CH_2), 1.44 (s, 9H, (CH_3)₃). ^{13}C NMR (100 MHz, CDCl_3): 173.88 (Cq), 173.03 (Cq), 167.71 (Cq), 166.57 (Cq), 165.44 (Cq), 143.54 (Cq), 137.74 (Cq), 131.37 (Cq), 120.15 (C (aromatic)), 81.47 (Cq), 79.37 (d, CH), 75.08 (CH_2), 71.12 (CH_2), 69.44 (CH_2), 69.40 (CH_2), 69.29 (CH_2), 69.10 (CH_2), 67.82 (CH_2), 58.36 (CH_2), 54.25 (CH_2), 38.98 (CH_2), 31.72 (CH_2), 28.01 (CH_3), 20.49 (CH_3). MS (ESI):

HRMS (ESI): (m/z): calcd for $C_{35}H_{46}N_2O_9+H$: 695.3027, found: 695.3052. $[\alpha]_D^{25} = -40$ ($c = 0.0025$, CH_2Cl_2).

Synthesis of cyclo[N²-(L- α -aspartyl-D-phenylalanyl)-N⁶-(N-(3,6,9,12-tetraoxapentadec-14-yn-1-yl)-N²-[(3,4,5-trihydroxyphenyl)carbonyl]-L- α -glutaminyl)-L-lysyl-N⁵-[amino(iminio)methyl]-L-ornithylglycyl] (11). *tert*-Butyl N-3,6,9,12-tetraoxapentadec-14-yn-1-yl-N²-{[3,4,5-tris(acetyloxy)phenyl] carbonyl}-L- α -glutamate **8** (100 mg, 0.14 mmol, 1 equiv) was treated with a solution of 4 M HCl in dioxane (4 mL) at 0 °C. After 15 min the reaction mixture was allowed to reach rt and was stirred for 4 h. The solvent was removed under reduced pressure and HCl was coevaporated three times with Et₂O to afford the intermediate carboxylic acid **9** (mass: 87 mg, yield: 95%). N-3,6,9,12-tetraoxapentadec-14-yn-1-yl-N²-{[3,4,5-tris(acetyloxy)phenyl]carbonyl}-L- α -glutamine **9** (35 mg, 0.05 mmol, 1 equiv) and PyBOP (34 mg, 0.07 mmol, 1.2 equiv) were dissolved in dry DCM (0.4 mL) at 0 °C. After 15 min, a solution of cyclo[Arg(Pbf)-Gly-Asp(OtBu)-D-Phe-Lys] **1** (50 mg, 0.05 mmol, 1 equiv) in DCM (0.5 mL) containing (*i*-Pr)₂NEt (20 μ L, 0.11 mmol, 2 equiv) was added to the reaction mixture at 0 °C. The reaction mixture was stirred for 2 h at rt. The product was concentrated under reduced pressure and purified by flash column chromatography (DCM/MeOH (9:1)). The resulting intermediate was dissolved in a solution of TFA/water (1.2 mL/0.08 mL) at rt. Triisopropylsilane (37 μ L) was added. The reaction mixture was stirred until total deprotection of cRGDFK peptide. The solution was concentrated under reduced pressure and the residue was dissolved in EtOH (0.1 mL). The reaction mixture was cooled to 0 °C and hydrazine (1.22 μ L, 0.025 mmol, 3 equiv) in EtOH (0.1 mL) was added. The reaction mixture was stirred for 30 min at 0 °C, concentrated under reduced pressure, and purified by HPLC (XTerra Prep RP C18, 19 \times 150 mm, Waters) to give the desired product (**11**) as a dark oil (mass: 10 mg, yield: 18% for 3 steps). IR (film): 3255, 2570, 1650, 1615, 1525, 1450, 1470, 1395, 1380, 1355, 1285, 1220, 1155, 1135, 1105, 910, 840, 780, 755, 740, 655, 590, 565, 535, 520 cm^{-1} . HRMS (ESI): (m/z): calcd for $C_{50}H_{71}N_{11}O_{17}+H$: 1098.5108, found: 1098.5106. $[\alpha]_D^{25} = -38$ ($c = 0.004$, CH_2Cl_2).

Materials. Preparation of the Bioceramics. Alumina was obtained from Ceralox (HPA-0.5, Sasol North America Inc., Tucson, AZ, USA). Hydroxyapatite (HA) (CAS 1306-06-5, purum p. a.) and β -tricalcium phosphate (TCP) (CAS 7758-87-4, purum p. a.) were purchased from Fluka (Switzerland). Dense bioceramic disks were prepared. For each disk, 4.5 g of HA or of TCP, or 6.2 g of alumina powders were filled into a cylindrical metallic matrix with a 30 mm inner diameter. TCP powder was gently sprayed with water before filling the matrix. The powders were unidirectionally compressed for 1 min at 15 kN in the case of alumina and HA and at 20 kN in the case of TCP. Then, the precompressed disks were isostatically pressed at 800 kN for 4 min to reach maximum green density. Sintering of the disks was carried out according to the following sintering schedules. In the case of HA and TCP: 1 °C/min from rt to 1200 °C, 6 h dwell time at 1200 °C, 3 °C/min from 1200 °C to rt. In the case of alumina: 1 °C/min from rt to 1575 °C, 2 h dwell time at 1575 °C, 3 °C/min from 1575 °C to rt.

Functionalization of the Bioceramics for XPS Measurements. A small fragment of each material (ca. 0.1 cm^3) was incubated in 1 mL of a 1 mM aqueous solution of the corresponding linker (**12a**, **b**, or **c**), at rt for 16 h, in the dark. The materials were drained on a piece of absorbent paper before being soaked in fresh water (1.5 mL) for 5 min to remove the nonattached linker. This procedure was repeated three times and the samples were then dried under a vacuum for 24 h and subsequently analyzed by XPS. XPS data were collected by an Axis Ultra instrument (Kratos analytical, Manchester, UK) under ultrahigh vacuum conditions ($<10^{-8}$ Torr) and using a monochromatic Al K α X-ray source (1486.6 eV).

Stability of the Chemical Coating on Bioceramics. A small fragment of each material (ca. 0.1 cm^3) was incubated in 1 mL of a 1 mM aqueous solution of compound **12c**, at rt for 16 h, in the dark. The materials were drained on a piece of absorbent paper before being soaked in fresh water (1.5 mL) for 5 min to remove the nonattached linker. This procedure was repeated three times and the samples were then dried under a vacuum for 24 h. The samples were then incubated

in Dulbecco's Modified Eagle medium (DMEM) supplemented with 10% fetal calf serum (FCS) for periods of 1 day and 14 days. The samples were drained on a piece of absorbent paper before being soaked in fresh water (1.5 mL) for 5 min to remove the released compound. This procedure was repeated three times and the samples were then dried under a vacuum for 24 h and subsequently analyzed by XPS. XPS data were collected by an Axis Nova instrument (Kratos analytical, Manchester, UK) under ultrahigh vacuum conditions ($<10^{-8}$ Torr) and using a monochromatic Al K α X-ray source (1486.6 eV).

Cellular Assays. Cells and Cell Culture Reagents. HUVEC were obtained from PromoCell (PromoCell, Heidelberg, Germany) and grown in Endothelial Cell Growth medium 2 (PromoCell) containing 10% heat-inactivated fetal calf serum (FCS), penicillin/streptomycin (Invitrogen, Basel, Switzerland) and supplemented with 2.5 mL of SupplementMix (PromoCell). The human lung A549 adenocarcinoma cell line is available from ATCC (American Tissue Culture Collection, Manassas, VA, USA). The cells were grown in Dulbecco's Modified Eagle Medium (DMEM) containing 4.5 g/L glucose, 10% FCS, and penicillin/streptomycin.

Immunofluorescence Staining for the $\alpha_v\beta_3$ Integrin. Cells were grown for 24 h on a glass slide (Gerhard Menzel, Braunschweig, Germany), fixed with a 4% PBS-buffered paraformaldehyde solution containing 1% sucrose, 1 mM CaCl₂, 1 mM MgCl₂, and 0.1% NaN₃ at 4 °C for 45 min. The cells were washed twice in PBS and permeabilized with methanol at -20 °C for 10 min at 4 °C. Two additional washings with PBS were performed followed by incubation of the cells in 5% BSA (Sigma-Aldrich, Buchs, Switzerland) in PBS containing 1 mM CaCl₂, 1 mM MgCl₂, and 0.1% NaN₃ at rt for 1 h. After two washings with PBS, the cells were incubated overnight at 4 °C with a murine antihuman $\alpha_v\beta_3$ integrin monoclonal antibody (Millipore, Billerica, USA; dilution 1:150) in HBSS (Invitrogen) containing 3% BSA, 0.1% Tween 20, and 0.1% NaN₃ (complete HBSS). The cells were washed three times with PBS for 5 min and incubated at rt under slight agitation with the secondary fluorescent antibody (antimouse Alexafluor 488 conjugate antibody, Invitrogen; dilution 1:250) in complete HBSS. The cells were washed three times with PBS for 5 min and the cell nuclei were labeled with a solution of 4',6-diamidino-2-phenylindole (DAPI, Roche Diagnostics, Rotkreuz, Switzerland, 1 μ g/mL in PBS) at rt for 5 min. A final washing with PBS was performed, and the evaluation of the $\alpha_v\beta_3$ integrin expression was evaluated by fluorescence microscopy (Zeiss Axioplan 2, filters: $\lambda_{ex}/\lambda_{em}$ 450–490/515–565 for Alexafluor 488; 365/420, for DAPI).

Evaluation of Vinculin and Cytoskeletal Actin after Incubation of the HUVEC with Compound 2. Cells were grown for 24 h in BD Falcon CultureSlides (BD Biosciences, Erembodegem, Belgium), then exposed to increasing concentrations (0 to 10 μ M) of compound **2** for 45 min at 37 °C in HBSS containing 0.1% BSA. The medium was removed and the cells were washed twice with PBS, fixed in 4% buffered paraformaldehyde for 10 min at rt. After two washings with PBS, the cells were incubated for 5 min in 0.1% PBS-Triton. Two additional washings with PBS were performed followed by incubation of the cells in PBS containing 5% BSA at rt for 1 h. Then, the cells were incubated overnight at 4 °C with a murine antivinculin monoclonal antibody (Invitrogen, dilution 1:300) in a solution for primary antibody (Calbiochem, Merck Biosciences, Darmstadt, Germany). The cells were washed three times with PBS for 5 min and incubated at rt for 1 h under slight agitation with a secondary fluorescent antimouse Rhodamine C-conjugated antibody (Invitrogen; dilution 1:250) in a solution for secondary antibody (Calbiochem). The cells were washed three times with PBS for 5 min and the cell nuclei and cytoskeletal actin were labeled with a solution of DAPI (1 μ g/mL in PBS) and 2.5% Oregon Green 488 Phalloidin (Invitrogen) at rt for 30 min. The cells were washed twice in PBS, and then the chamber was removed from the glass slide with the chamber removal device and the expression of vinculin and actin was evaluated by fluorescence microscopy (Zeiss Axioplan 2, filters: $\lambda_{ex}/\lambda_{em}$ 450–490/515–565 for Oregon Green 488; 365/420, for DAPI; 510–560/590 for Rhodamine C).

HUVEC Labeling with Compound 2. Cells were grown for 24 h on BD Falcon CultureSlides (BD Biosciences) and then exposed to increasing concentrations (0–10 μ M) of either compound 2 or free biotin (Sigma-Aldrich), for 30 min at 37 °C, in HBSS containing 0.1% BSA. The medium was removed and the cells were washed twice with PBS, fixed in 4% buffered formaldehyde for 10 min at rt. After two washings with PBS, the cells were labeled by incubation with streptavidin-Alexafluor 488 (Invitrogen, dilution 1:2000, 2 mg/mL) in PBS containing 1% BSA at rt for 30 min, in the dark. After two additional washings with PBS, the cell nuclei were labeled with DAPI (1 μ g/mL in PBS) at rt for 5 min, in the dark. The cells were washed twice in PBS, and then the chamber was removed from the glass slide and the evaluation of cell recognition was performed by fluorescence microscopy (Zeiss Axioplan 2, filters: $\lambda_{ex}/\lambda_{em}$ 450–490/515–565 for Alexafluor 488; 365/420, for DAPI).

HUVEC Labeling with Ligand 11. Cells were grown for 24 h on BD Falcon CultureSlides (BD Biosciences) and then exposed to increasing concentrations of ligand 11 in HBSS containing 0.1% BSA, for 3 h at 37 °C. The medium was removed and the cells were washed twice with PBS, fixed in 4% buffered formaldehyde for 10 min at rt. After two washings with PBS, the cells were labeled by click reaction using Alexafluor 488-azide (Invitrogen, 10 μ M), CuSO₄ (Sigma-Aldrich, 2 mM), and sodium ascorbate (Sigma-Aldrich, 1 mM) in PBS containing 1% of BSA, at rt for 30 min, in the dark. After two washings with PBS, the cell nuclei were labeled with DAPI (1 μ g/mL in PBS) at rt for 5 min, in the dark. The cells were washed twice in PBS, and then the chamber was removed from the glass slide and the evaluation of the cell recognition was performed by fluorescence microscopy (Zeiss Axioplan 2, filters: $\lambda_{ex}/\lambda_{em}$ 450–490/515–565 for Alexafluor 488; 365/420, for DAPI).

Adhesion of HUVEC on the Bioceramics. Disks ($d = 2.5$ cm, $h = 0.5$ cm) of each of the three bioceramics were incubated in a solution of ligand 11 at increasing concentrations (0, 2.5, 5, and 10 μ M) for 24 h at rt, in the dark under slight stirring. The disks were washed three times with water and dried under a vacuum for 24 h. HUVEC were trypsinized, counted, and centrifuged for 5 min after dilution in HBSS. Three mL of the cell suspension (100 000 cells/mL) were added on the disks of unfunctionalized or functionalized bioceramics in a six-well plate (Costar, Corning, NY, USA) and incubated for 2 h at 37 °C. The media were removed. The disks were washed once with PBS and inserted in a new well, fixed with 4% buffered formaldehyde for 10 min at rt, and then stained in a solution of crystal violet (Sigma-Aldrich, 1.5% glacial acetic acid, 0.05% crystal violet in water), for 5 min at rt. Adhered cells were imaged by stereomicroscopy (MZ16 FA Leica/DFC 480 Leica, 0.63X and 1.6X, zoom 72X) and the cell number and surface areas were evaluated using the Image J software. The cell surface areas were then represented by a Boxplot.

Western Blotting Experiments of Bioceramic-Desorbed Human Plasma Proteins. Fresh human blood in serum separation-containing gel tubes (BD Falcon, Erembodegem, Belgium) was obtained from leftovers of analytical blood with normal values. Tubes were centrifuged for 10 min at 4000 rpm and serum was collected from the upper phase. Disks of unfunctionalized and functionalized bioceramics with ligand 11 were incubated with human serum at 37 °C, for 1 h under slight agitation, then washed three times with PBS and proteins adsorbed on the materials were solubilized in boiling SDS buffer (50 mM Tris buffer, 2% SDS, 5% β -mercaptoethanol), for 30 min under agitation. Desorbed proteins were resolved by SDS–PAGE (6% and 8% polyacrylamide gels) and transferred onto a nitrocellulose membrane (Whatman, Dassel, Germany) and then blotted with rabbit polyclonal antihuman fibronectin (Millipore, diluted 1:5000), antihuman vitronectin (Santa Cruz Biotechnology, Heidelberg, Germany, diluted 1:5000), antihuman IgG (Dako, Glostrup, Denmark, diluted 1:2000), or mouse monoclonal antihuman fibrinogen (Abcam, Cambridge, UK, diluted 1:1000) antibodies. The membrane was exposed for 60 min to horseradish peroxidase-conjugated antirabbit (Sigma-Aldrich) or antimouse (Sigma-Aldrich) antibodies (diluted 1:5000) and visualized by enhanced chemiluminescence (ECL, GE Healthcare, Amersham, UK).

Statistical Analysis. Results were subjected to computer-assisted statistical analysis using the R and RStudio softwares. The distribution of data was tested by the Shapiro-Wilk test. The data that were from a normally distributed population were compared using the Student's *t*-test, whereas data not normally distributed were compared using the Wilcoxon signed-rank test. Differences of $p < 0.05$ were considered significant.

■ ASSOCIATED CONTENT

⑤ Supporting Information

Evaluation of microbial contamination of the bioceramics. Evaluation of the total adsorption of human serum proteins. Evaluation of the stability of the chemical coating on bioceramics in cell culture medium. Detailed chemical syntheses: Synthesis of cyclo[Arg(Pbf)-Gly-Asp(OtBu)-D-Phe-Lys(Z)] (1); synthesis of cyclo(Arg-Gly-Asp-D-Phe-Lys)-Biotin (2); synthesis of *tert*-butyl N-3,6,9,12-tetraoxapentadec-14-yn-1-yl-*N*²-{[3,4,5-tris(acetyloxy)phenyl]carbonyl}-*L*- α -glutamate (8); synthesis of cyclo{*N*²-(*L*- α -aspartyl-D-phenylalanyl)-*N*⁶-{N-(3,6,9,12-tetraoxapentadec-14-yn-1-yl)-*N*²-[(3,4,5-trihydroxyphenyl)carbonyl]-*L*- α -glutaminy]}-*L*-lysyl-*N*²-[amino(iminio) methyl]-*L*-ornithylglycyl} (11). This material is available free of charge via the Internet at <http://pubs.acs.org>.

■ AUTHOR INFORMATION

Corresponding Author

* (L.J.-J.) Address: University Institute of Pathology, CHUV-UNIL rue du Bugnon 25; CH-1011 Lausanne, Switzerland. Phone: +41 21 314 7173; fax: +41 21 314 7115; e-mail: lucienne.juillerat@chuv.ch (S.G.-L.) Address: Laboratory of Synthesis and Natural Products; Ecole Polytechnique Fédérale de Lausanne (EPFL), ISIC, Batochime, CH-1015 Lausanne, Switzerland. Phone: +41 21 693 93 72; fax: +41 21 693 93 55; e-mail: Sandrine.Gerber@epfl.ch.

Notes

The authors declare no competing financial interest.

■ ACKNOWLEDGMENTS

We thank the Swiss National Science Foundation (Grant Nos. CR2313-124753 and CR2212-140866) for financial support, Dr. L. Menin, J. Artacho, M. Rey, Dr. P. Miéville, F. Sepulveda, and C. Chapis Bernasconi for excellent technical support and M. Federico Tettamanti for the statistical advices.

■ ABBREVIATIONS USED

DAPI, 4',6-diamidino-2-phenylindole; DMEM, Dulbecco's modified Eagle medium; FCS, fetal calf serum; HA, hydroxyapatite; HBSS, Hank's buffered salt solution; HEPE, 4-(2-hydroxyethyl)-1-piperazineethanesulfonic acid; HUVEC, human umbilical vein endothelial cells; OSu, oxy succinimide; Pbf, 2,2,4,6,7-pentamethylidihydrobenzofuran-5-sulfonyl; PyBOP, benzotriazol-1-yl-oxytripyrrolidinophosphonium hexafluorophosphate; RGD, arginine-glycine-aspartate; TCP, tricalciumphosphate; XPS, X-ray photoelectron spectroscopy

■ REFERENCES

- (1) Ghanaari, S.; Unger, R. E.; Webber, M. J.; Barbeck, M.; Orth, C.; Kirkpatrick, J. A.; Booms, P.; Motta, A.; Migliaresi, C.; Sader, R. A.; Kirkpatrick, C. J. Scaffold Vascularization *in vivo* Driven by Primary Human Osteoblasts in Concert with Host Inflammatory Cells. *Biomaterials* 2011, 32, 8150–8160.
- (2) Perets, A.; Baruch, Y.; Weisbuch, F.; Shoshany, G.; Neufeld, G.; Cohen, S. Enhancing the Vascularization of Three-Dimensional

Porous Alginate Scaffolds by Incorporating Controlled Release Basic Fibroblast Growth Factor Microspheres. *J. Biomed. Mater. Res. A* **2003**, *65*, 489–497.

(3) Geiger, F.; Bertram, H.; Berger, I.; Lorenz, H.; Wall, O.; Eckhardt, C.; Simank, H.-G.; Richter, W. Vascular Endothelial Growth Factor Gene Activated Matrix (VEGF165-GAM) Enhances Osteogenesis and Angiogenesis in Large Segmental Bone Defects. *J. Bone Miner. Res.* **2005**, *20*, 2028–2035.

(4) Ghanaati, S.; Webber, M. J.; Unger, R. E.; Orth, C.; Hulvat, J. F.; Kiehna, S. E.; Barbeck, M.; Rasic, A.; Stupp, S. I.; Kirkpatrick, C. J. Dynamic In Vivo Biocompatibility of Angiogenic Peptide Amphiphile Nanofibers. *Biomaterials* **2009**, *30*, 6202–6212.

(5) Rajangam, K.; Behanna, H. A.; Hui, M. J.; Han, X.; Huivat, J. F.; Lomasney, J. W.; Stupp, S. I. Heparin Binding Nanostructures to Promote Growth of Blood Vessels. *Nano Lett.* **2006**, *6*, 2086–2090.

(6) Elbjeirami, W. M.; West, J. L. Angiogenesis-like Activity of Endothelial Cells Co-Cultured with VEGF-Producing Smooth Muscle Cells. *Tissue Eng.* **2006**, *12*, 381–390.

(7) Ribatti, D.; Nico, B.; Morbidelli, L.; Donnini, S.; Ziche, M.; Vacca, A.; Roncali, L.; Presta, M. Cell-Mediated Delivery of Fibroblast Growth Factor-2 and Vascular Endothelial Growth Factor onto the Chick Chorioallantoic Membrane: Endothelial Fenestration and Angiogenesis. *J. Vasc. Res.* **2001**, *38*, 389–397.

(8) Hubbel, J. A. Materials as Morphogenetic Guides in Tissue Engineering. *Curr. Opin. Biotechnol.* **2003**, *14*, 551–558.

(9) Kim, B. S.; Mooney, D. J. Development of Biocompatible Extracellular Matrices for Tissue Engineering. *Trends Biotechnol.* **1998**, *16*, 224–230.

(10) Lutolf, M. P.; Hubbel, J. A. Synthetic Biomaterials as Instructive Extracellular Microenvironments for Morphogenesis in Tissue Engineering. *Nat. Biotechnol.* **2005**, *23*, 47–55.

(11) Fuchs, S.; Motta, A.; Migliaresi, C.; Kirkpatrick, C. J. Outgrowth Endothelial Cells Isolated and Expanded from Human Peripheral Blood Progenitor Cells as a Potential Source of Autologous Cells for Endothelialisation of Silk Fibroin Biomaterials. *Biomaterials* **2006**, *27*, 5399–5408.

(12) Santos, M. I.; Fuchs, S.; Gomes, M. E.; Unger, R. E.; Reis, R. L.; Kirkpatrick, C. J. Response of Micro- and Macrovascular Endothelial Cells to Starch-based Fiber Meshes for Bone Tissue Engineering. *Biomaterials* **2007**, *28*, 240–248.

(13) Santos, M. I.; Tuzlakoglu, K.; Fuchs, S.; Gomes, M. E.; Peters, K.; Unger, R. E.; Piskin, E.; Reis, R. L.; Kirkpatrick, C. J. Endothelial Cell Colonization and Angiogenic Potential of Combined Nano- and Micro-Fibrous Scaffolds for Bone Tissue Engineering. *Biomaterials* **2008**, *29*, 4306–4313.

(14) Hennessy, K. M.; Clem, W. C.; Phipps, M. C.; Sawyer, A. A. The Effect of RGD Peptides on Osteointegration of Hydroxyapatite Biomaterials. *Biomaterials* **2008**, *29*, 3075–3083.

(15) Bellis, S. Advantages of RGD Peptides for Directing Cell Association with Biomaterials. *Biomaterials* **2011**, *32*, 4205–4210.

(16) Borcard, F.; Godinat, A.; Staedler, D.; Comas Blanco, H.; Dumont, A.-L.; Chapuis-Bernasconi, C.; Applegate, L. A.; Krauss Juillerat, F.; Gonzenbach, U. T.; Gerber-Lemaire, S.; Juillerat-Jeanneret, L. Covalent Cell Surface Functionalization of Human Fetal Osteoblasts for Tissue Engineering. *Bioconjugate Chem.* **2011**, *49*, 689–692.

(17) Comas, H.; Laporte, V.; Borcard, F.; Krauss Juillerat, F.; Gonzenbach, U. T.; Juillerat-Jeanneret, L.; Gerber-Lemaire, S. Surface Functionalisation of Alumina Ceramic Foams with Organic Ligands. *Appl. Mater. Interfaces* **2012**, *4*, 573–576.

(18) Fields, G. B.; Noble, R. L. Solid-phase Peptide Synthesis Utilizing 9-Fluorenylmethoxycarbonyl Amino Acids. *Int. J. Pept. Protein Res.* **1990**, *35*, 161–214.

(19) Sabra, G.; Vermette, P. Endothelial Cell Responses Towards Low-Fouling Surfaces Bearing RGD in a Three-Dimensional Environment. *Exp. Cell. Res.* **2011**, *317*, 1994–2006.

(20) Pasqualini, R.; Koivunen, E.; Ruoslahti, E. Alpha v Integrins as Receptors for Tumor Targeting by Circulating Ligands. *Nat. Biotechnol.* **1997**, *15*, 542–546.

(21) Marinelli, L.; Lavecchia, A.; Gottschalk, K. E.; Novellino, E.; Kessler, H. Docking Studies on Alpha_vBeta₃ Integrin Ligands: Pharmacophore Refinement and Implications for Drug Design. *J. Med. Chem.* **2003**, *46*, 4393–4404.

(22) Dos Santos, E. A.; Farina, M.; Soares, G. A.; Anselme, K. Surface Energy of Hydroxyapatite and β -Tricalcium Phosphate Ceramics Driving Serum Protein Adsorption and Osteoblast Adhesion. *J. Mater. Sci.* **2008**, *19*, 2307–2316.